

Neutron diffraction, magnetization, and ESR studies of pseudocubic $\text{Nd}_{0.75}\text{Ba}_{0.25}\text{MnO}_3$ and its critical behavior above T_C

V. A. Ryzhov, A. V. Lazuta, O. P. Smirnov, I. A. Kiselev, Yu. P. Chernenkov, and S. A. Borisov
Petersburg Nuclear Physics Institute, Gatchina, Leningrad District, 188300, Russia

I. O. Troaynchuk and D. D. Khalyavin
Institute of Physics of Solids and Semiconductors, National Academy of Sciences, ul. P. Brovki street 17, Minsk, 220072, Belarus
 (Received 18 February 2005; revised manuscript received 18 August 2005; published 27 October 2005)

Results of structural neutron diffraction study, magnetization, and electron spin resonance (ESR) measurements are presented for insulating $\text{Nd}_{1-x}\text{Ba}_x\text{MnO}_3$ ($x=0.25$) with the Curie temperature $T_C \approx 129$ K. Detailed analysis of the data is performed by using $Pbnm$ space group in a temperature range 4.2–300 K. The compound is found to exhibit the Jahn-Teller (JT) transition at $T_{JT} \sim 250$ K. The character of the coherent JT distortions and their temperature evolution differ from those of the $x=0.23$ manganite. The field cooled magnetization data are in reasonable agreement with the predictions for a three-dimensional (3D) isotropic ferromagnet above T_C . These measurements, however, reveal a difference between the field cooled and zero field cooled data in the paramagnetic region. The ESR results also correspond with behavior of a 3D isotropic ferromagnet above $T^* \approx 143$ K [$\tau^* \approx 0.12 \leq \tau < 1$, $\tau = (T - T_C)/T_C$]. The T -dependence of the ESR linewidth is found to be proportional to $[T\chi(T)]^{-1}$, where $\chi(T)$ is the susceptibility. This uncritical behavior results from the anisotropic spin interactions that can be attributed to the Dzyaloshinsky-Moria (DM) coupling. The critical enhancement is not observed. It can be explained by the strong uncritical contribution to the linewidth, and suppression of the critical enhancement by a magnetic field. The different temperature treatments (slow/fast cooling/heating, with/without external magnetic field) of the sample reveal a temperature hysteresis of the ESR spectra below T^* indicating an anomalous response in the paramagnetic region. The study of the magnetic phase transition in the $x=0.23$ and 0.25 manganites suggests change in its character from second to first order at T^* . The conventional free energy including the magnetization and magnetic field is not found to describe this first order transition. This suggests that the charge, orbital, and JT phonon degrees of freedom, in addition to magnetization, may be the critical variables, the unusual character of the transition being determined by their coupling. The unconventional critical behavior is attributed to an orbital liquid metallic phase that begins to coexist with the initial orbital ordered phase below T^* .

DOI: [10.1103/PhysRevB.72.134427](https://doi.org/10.1103/PhysRevB.72.134427)

PACS number(s): 75.60.Ej, 61.12.Ld, 75.40.Cx, 75.40.Gb

I. INTRODUCTION

Doped manganites $L_{1-x}A_x\text{MnO}_3$ (L and A are rare earth and alkaline earth ions, respectively) usually exhibit the ferromagnetic (F) ground state in a region $x_0 \leq x \leq 0.5$. In $\text{Nd}_{1-x}\text{Ba}_x\text{MnO}_3$, this state develops below $T_C \sim 120$ K for $0.2 \leq x \leq 0.35$.¹ For $x < 0.3$, these compounds show insulating (I) behavior in the ordered state, whereas for $x \geq 0.3$ the F metallic (M) state is observed below T_C . A colossal magnetoresistance occurs for all x near T_C . The unexpected coexistence of ferromagnetic and insulating behavior cannot be explained by the double exchange mechanism and remains poorly understood. A possible reason of the charge localization can be a long-range orbital ordering due to the Jahn-Teller (JT) effect. This source of the localization was suggested to account for the ferromagnetic insulating (FI) ground state in $\text{La}_{1-x}\text{Ca}_x\text{MnO}_3$ for $0.12 < x < 0.2$.² The FI state can also be a consequence of a spontaneous orbital ordering, which develops in a cubic manganite, due to a coupling of the spin and orbital degrees of freedom arising from the electron correlations.³ $\text{La}_{0.88}\text{Sr}_{0.12}\text{MnO}_3$ was found to exhibit the FI state of such nature.⁴ Note that an explanation of the insulator to metal transition, which occurs in an orbital disordered state, has been suggested recently.⁵ This

approach permits the existence of an orbital liquid insulating state. As far as we know, however, such a state has not been found so far.

An important aspect of this problem is the nature of the paramagnetic (P) -FI transition which can differ from that of a 3D isotropic ferromagnet. A few works have only concentrated on behavior at this critical point. An unconventional P-FI transition was observed in insulating $\text{La}_{0.8}\text{Ca}_{0.2}\text{MnO}_3$ where a magnetic correlation length increased only from 10 to 35 Å as $T \rightarrow T_C$.⁶ To investigate this issue in detail, we have used $\text{Nd}_{1-x}\text{Ba}_x\text{MnO}_3$ compounds, which are closed to the cubic perovskites due to the small structural distortions.¹ Our studies have included the measurements of the linear and nonlinear susceptibilities as well as ESR. The neutron diffraction investigations have been also performed to elucidate the effects of the lattice distortions and orbital ordering. The study of the critical magnetic properties of the $x=0.23$ ($T_C \approx 124$ K) and $x=0.25$ ($T_C \approx 129$ K) manganites revealed a more complicated scenario than that expected for the 3D isotropic ferromagnets.⁷⁻¹⁰ The conventional critical behavior was observed to proceed for $T^* < T < 2T_C$, where $T^* \approx 147$ K ($x=0.23$) and $T^* \approx 143$ K ($x=0.25$). In contrast, the data on nonlinear response of the second order clearly indicated the occurrence of an anomalous critical behavior

for $T_C < T < T^*$ that suggested the coexistence of the two magnetic phases. Although the $x=0.23$ compound exhibited an orbital ordering due to the JT effect below $T_{JT} \sim 350$ K, the neutron diffraction study did not reveal a two phase structure in the anomalous T range⁹ that would be a natural explanation of the phase separated (PS) magnetic state. In addition, according to the ESR measurements, the transition did not become hysteretic in temperature and clearly first order.

In this paper we present the neutron diffraction, magnetization, and ESR investigations of $x=0.25$ manganite. These studies are performed to elucidate a reason of the anomalous critical behavior found in the measurements of the second harmonic of magnetization, M_2 .¹⁰ The neutron diffraction provides important information on structural change at phase transitions while two other methods are traditionally used for an analysis of the magnetic ones. The ESR has been applied to examine the critical behavior at the higher steady magnetic field H and frequency ($f \approx 8.37$ GHz) than in previous M_2 experiments ($f \approx 15.7$ MHz, $H \leq 300$ Oe). To analyze correctly the critical dynamics in a steady magnetic field (ESR) one needs the data on corresponding static behavior (magnetization). According to structural data the T_{JT} is reduced on doping, becoming $T_{JT} \sim 250$ K. A character of the JT distortions and orbital ordering differs from that of the $x=0.23$ compound. T evolution of the structural parameters does not show any anomalies that can be definitely attributed to formation of a structural PS state in the anomalous T range. The magnetization, $M(H)$, measurements are performed in the field cooled (FC) and zero field cooled (ZFC) regimes at $H=1$ kOe in a range 4.2–300 K. The FC data agree reasonably with predictions for a 3D isotropic ferromagnet in the paramagnetic critical region from $2T_C$ down to T_C . At the same time, a difference between the FC and ZFC results is unexpectedly found to proceed up to 300 K. ESR measurements are carried out above T_C . A relaxation rate of uniform magnetization Γ and the g factor show nearly the same dependencies above T^* as for the $x=0.23$ manganite. The $\Gamma(\tau)$ does not exhibit a critical enhancement in contrast to the conventional cubic ferromagnets CdCr_2S_4 and CdCr_2Se_4 .¹¹ It reveals the pure uncritical behavior that can be related to the Dzyaloshinsky-Moria (DM) interaction. The strong uncritical relaxation mechanism and suppression of the critical broadening by a magnetic field are shown to be the probable reasons of the lack of observation of the critical enhancement. In order to examine a character of the phase transition, the effect of the different temperature treatments of the sample on the ESR signals is elucidated. These measurements and $M(H)$ data support the existence of the magnetic PS state near T_C . The possible reasons of origination of the heterophase magnetic state are discussed.

II. SAMPLES AND METHODS

The polycrystalline samples were prepared by the standard technology,¹ an oxygen content being controlled by a thermogravimetric analysis. Single crystals of $\text{Nd}_{1-x}\text{Ba}_x\text{MnO}_3$ ($x \approx 0.25$) were grown by the flux melt technique using the $\text{BaO-B}_2\text{O}_3\text{-BaF}_2$ ternary system as a

solvent.¹² The cation composition of the crystals was determined by x-ray fluorescent analysis based on the relation of K_αNd and K_αBa lines of secondary characteristic radiation spectra. The perturbation of the main elements were realized by ^{241}Am ($\gamma=59.54$ keV) radioisotope source. The x-ray spectrometer provided by an Si(Li)-semiconductor detector was used to register the secondary characteristic radiation with 200 eV accuracy at 5.95 keV line from ^{55}Fe radioisotope source. The average oxidation state of manganese determined by photometry¹³ was found to be close to the value expected for the stoichiometric oxygen content. The following composition was detected for the crystal: $\text{Nd}_{0.745(5)}\text{Ba}_{0.255(5)}\text{Mn}_{1.0(1)}\text{O}_{3.01(2)}$.

A 48-counter powder neutron diffractometer of PNPI with a wave length 1.83 Å of an incident neutron beam was used in the structural investigations. The measurements were performed in a cryostat at 4.2–300 K. The program FULLPROF was employed for the structure refinement.

The magnetization measurements were carried out using a superconducting quantum interference device (SQUID) magnetometer in a temperature range 4.2–300 K and a magnetic field 1 kOe. A single crystal with a mass $m=91.8$ mg was studied that came from the same growth batch as the crystal of work.¹⁰

In ESR experiments, the small part of single crystal investigated in work¹⁰ with a mass $m \approx 1.6$ mg was used. We employed a special X-band ESR spectrometer ($f=8.37$ GHz) described earlier.^{14,15} It registers a component of magnetization of a sample which is proportional to an off-diagonal part of its magnetic susceptibility [$M_y(\omega) = \chi_{yx}(\omega)h_x(\omega)$] when a linear polarized exciting ac field $\mathbf{h} \parallel \text{Ox}$ and a steady field $\mathbf{H} \parallel \text{Oz}$ and allows one to avoid the problem associated with absorption in zero field.

Below $T^* \approx 143$ K, the nonlinear response of the compound reveals features of the PS magnetic state that can signal the first order transition.¹⁰ It is natural, therefore, to expect a temperature hysteresis of the ESR signal. Besides, a state forming at the PS usually depends on a process that is used to transfer a system in the PS regime. Therefore, several types of the temperature scan with/without an external magnetic field were performed.

(a.) The sample was slowly cooled from room temperature down to 128 K below T_C and then slowly heated back to room temperature. In the chosen temperature points (T points) the ESR spectra were registered. A temporal stabilization time before recording a signal was about 200–300 s at each T point.

(b.) The same temperature scan as above was applied but with $H=4$ kOe during cooling between T points. This procedure also tests a possible PS state because the magnetic field can change a balance between the phase fractions.

(c.) A fast cooling of the sample was used down to 128 K in zero H and then the sample was slowly heated up to room temperature.

III. STRUCTURAL DATA

A neutron diffraction pattern at room temperature is plotted in Fig. 1. Similar to $\text{Nd}_{0.77}\text{Ba}_{0.23}\text{MnO}_3$ crystal,⁹ the

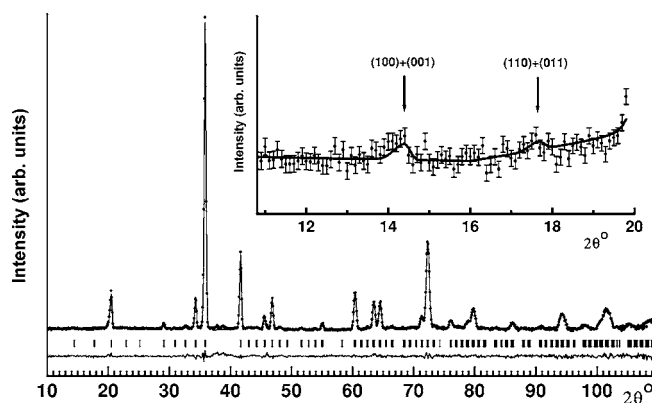


FIG. 1. The neutron diffraction pattern, calculated profile, and residual curve for $\text{Nd}_{0.75}\text{Ba}_{0.25}\text{MnO}_3$ at room temperature. The inset shows the wide and weak monoclinic peaks at the small angles.

pseudocubic structure of $\text{Nd}_{0.75}\text{Ba}_{0.25}\text{MnO}_3$ exhibits distortions to a monoclinic symmetry as the characteristic peaks at the low angles of scattering evidence (see the insert in Fig. 1). They unambiguously originate from a lattice deformation because the x-ray diffraction patterns also show them at room temperature. A width of the peaks is larger than that of the main Bragg reflections. It indicates that the regions of the relatively small sizes possess the monoclinic distortions. The peaks exhibit no temperature variations and have a small amplitude. The presence of a small amount of such a monoclinic phase is expected to have a minimal effect on the T -dependent properties of this compound. The measured diffraction profiles are found to be well-fitted using the orthorhombic $Pbnm$ space group. This fit gives only a slightly worse description than that of the monoclinic group $P21/m$. Therefore, further analysis will be based on the $Pbnm$ setting. Figure 2 displays the T variations of structural parameters. The orthorhombic distortions are small in range of the measurements as in the $x=0.23$ manganite.⁹ However, there are essential differences in their character.

The data on the Mn-O bond lengths [Fig. 2(c)] indicate that the JT transition from the high temperature orbital disordered O phase to the O' phase possessing the cooperative JT distortions occurs at $T_{JT} \sim 250$ K. This transition involves the strong abrupt changes of the Mn-O-Mn angles between 220–290 K when the curves of monotonic T variation for the Mn-O1-Mn and Mn-O2-Mn angles cross one another [Fig. 2(d)]. This transformation is related to rotation of the MnO_6 octahedra around the pseudocubic $[111]$ direction.¹⁶ Thus, the OO' transition is driven by both the JT distortions that underlie an orbital ordering and a steric effect (the oxygen ion displacements connected to the octahedrons tilting). The latter leads to peculiarity of the transition when a relationship between the lattice parameters [$a > b \approx c/\sqrt{2}$, Fig. 2(a)] conserves above and below T_{JT} , the splitting $a-b$ becoming even smaller on cooling below T_{JT} . The OO' transition is not usually accompanied by the octahedral tilting. In this case $c/\sqrt{2} \approx a \approx b$ above T_{JT} and $c/\sqrt{2} < a, b$ below it, as it is found in LaSr ,¹⁶ LaCa ,¹⁷ and $x=0.23$ NdBa ⁹ manganites. The T variations of the lattice parameters and unit-cell volume [Figs. 2(a) and 2(b)] are observed above T_C . They mainly reflect compression of the lattice on cooling which is related

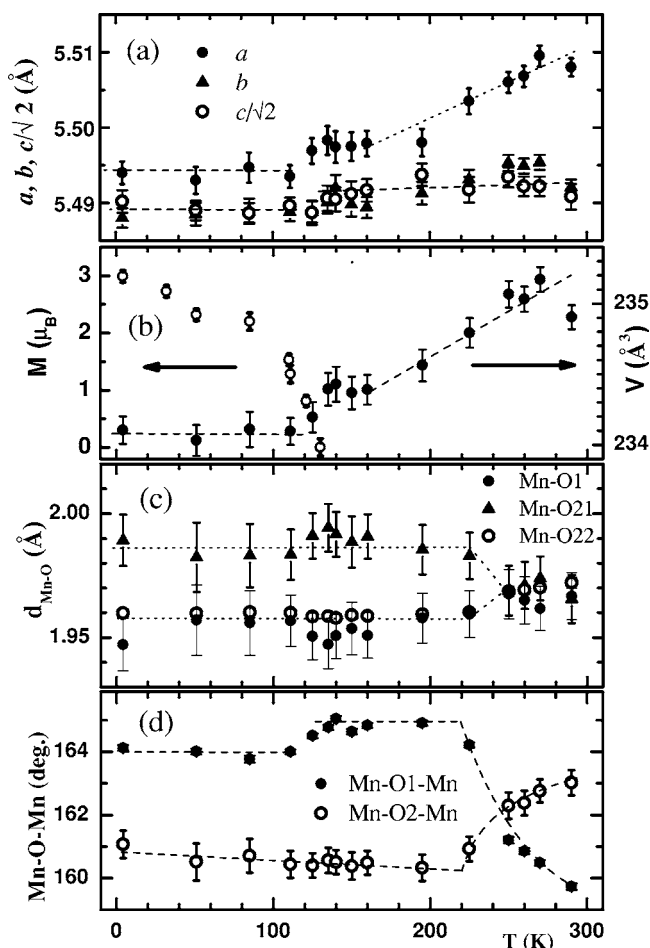


FIG. 2. Temperature dependences of the structural parameters a, b, c [panel (a)]; volume of the unit cell V and magnetic moment of the sample per Mn ion [panel (b)]; the Mn-O bond lengths [panel (c)]; and the Mn-O-Mn angles [panel (d)].

to reduction of the lattice parameter. This process completes at T_C . The Mn-O bond lengths [Fig. 2(c)] coincide above $T_{JT} \sim 250$ K and their splitting remains nearly temperature independent below 230 K, so that the JT phase forms in the narrow temperature interval. The splitting corresponds to the orbital ordering close to $3y^2 - r^2/3x^2 - r^2$ type which develops in the $a-b$ plane because $d\text{Mn-O1} \approx d\text{Mn-O22} > d\text{Mn-O21}$.¹⁶ In $\text{La}_{1-x}\text{Ca}_x\text{MnO}_3$ ($0.12 < x \leq 0.21$) with the FI ground state, the JT distortions monotonically increase on cooling over a large temperature interval.² At $x=0.2$, this behavior is observed from $T \approx 300$ K $> T_C \approx 170$ K down to 100 K. It was interpreted as the coexistence of the O and O' phases, i.e., as the structural PS state. Although our measurements of the $d\text{Mn-O}$ are not a very high accuracy, they contradict the coexistence of the O and O' phase with the comparable volume fractions even at 220 K, and support formation of the nearly structural uniform phase below 230 K. The T evolution of the structural parameters does not reveal any peculiarities in the anomalous T range ($T^* \approx 143$ K– 129 K $\approx T_C$) which can be directly associated with the appearance of a two-phase structural state. Note that a character of the JT distortions in the $x=0.23$ manganite below 150 K ($d\text{Mn-O21} - d\text{Mn-O1} \approx d\text{Mn-O1} - d\text{Mn-O22}$), where it depends

weakly on temperature,⁹ differs from that of the $x=0.25$ manganite. Thus, the FI state and the anomalous critical behavior can occur at the different types of these distortions.

Temperature dependence of the ferromagnetic moment [Fig. 2(b)] shows the usual behavior for a ferromagnet with $T_C \approx 129$ K. The value of T_C was determined previously from the data on a third harmonic of magnetization of a nonlinear response in a low frequency magnetic field.¹⁰ The magnetic moment in the ground state $3.0(1) \mu$ (μ is the Bohr magneton) is less than that of the Mn sublattice 3.75μ expected for this composition. This is most likely due to antiparallel alignment of the Nd magnetic moment that can give an additive contribution in measured ferromagnetic moment of the sample. This suggestion is in agreement with the magnetization behavior at low temperatures (see below). The statistics are not good enough to introduce a Nd magnetic subsystem in a model for refinement of the structural data and to determine the magnitudes and the directions of the Mn and Nd magnetic moments separately. At the same time, these properties were established for $x=0.3$ NdBa manganite¹⁸ which possesses a close to our compound crystal structure and the same F ground state. The Nd magnetic moment was observed below 50 K, directed antiparallel to the Mn moments, and equal to 0.5μ at 1.4 K.

IV. MAGNETIZATION

Figure 3 displays the temperature dependences of M that are obtained in the FC and ZFC measurements at $H = 1$ kOe. We consider first the FC data above T_C . To determine a scaling behavior of susceptibility of the material χ and to estimate a demagnetization factor, it is convenient to write inverse susceptibility of the sample $\chi_{\text{ext}}^{-1} = H/M$ as

$$\chi_{\text{ext}}^{-1} = \chi^{-1} + 4\pi N. \quad (1)$$

Here $\chi = C_\chi [S(S+1)/(3kT_C)] [(g\mu)^2/V_0] \tau^{-\gamma}$ (the conventional units), k is the Boltzmann constant, C_χ is the numerical factor, g is the g factor, $V_0 \approx 41.45 \text{ \AA}^3$ is the volume of the unit magnetic cell and N is the demagnetization factor. A fit of the data for $1 > \tau > 0.093$ ($258 \text{ K} > T > 141 \text{ K}$) with $T_C \approx 129$ K and $N=1/3$ gives $\gamma=1.39(1)$, $C_\chi=2.95(3)$ for $S=1.875$, these values being independent on N for $0.25 < N < 0.4$ [see inset (1) in Fig. 3]. The same values of γ and C_χ are obtained by employing an interval $1 > \tau > 0.256$ whereas the fit becomes worse approximately below 141 K. This shows that $H=1$ kOe affects the $\chi(\tau)$ dependence only at $\tau < 0.093$. The ac linear response¹⁰ and ESR measurements (see Fig. 5) give a slightly lesser value of $\gamma \approx 1.32$ that is due to the demagnetization effects because a fit of the $M/H = \chi_{\text{ext}}$ data yields also a close magnitude of γ .

Since the nonlinear response reveals the anomalous critical behavior in the low magnetic fields below $T^* \approx 143$ K, it is important to check whether the critical $M(\tau)$ dependence at $H=1$ kOe is the conventional one or not in the same T range. Our $M(\tau)$ data in this region are related mainly to an intermediate H regime between the weak ($T > 143$ K) and strong ($T=T_C$) magnetic fields. As can be easily verified, a modified Arrott plot scheme frequently employed for analy-

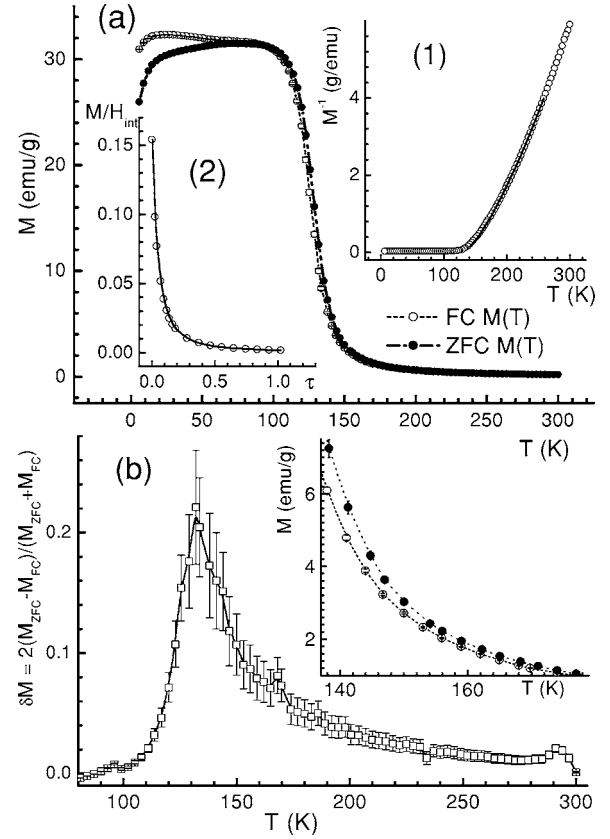


FIG. 3. Temperature dependence of the magnetization for the cooling and heating regimes under $H=1$ kOe. Panel (a) shows these dependencies in the full temperature range 6–300 K. Inset (1) displays fit of the $M^{-1}(T)$ measured in the ZFC regime to the function $\tau^\gamma/CH+4\pi N/H$. The fitting parameters are found to be $1/CH = 3.98(3) \text{ g/emu}$ and $\gamma=1.39(1)$ at $N=1/3$. Inset (2) represents fit of the ZFC $M(\tau)/H_{\text{int}}$ to expressions (2), (3) (see the text) in T range T_C-261 K. Panel (b) shows the relative difference δM vs T in the T range 80–300 K. The insert in (b) displays the $M(T)$ curves registered in the ZFC and FC regimes in T range 140–180 K.

sis of the critical $M(\tau, H)$ dependences^{19,20} has the incorrect analytic properties in the weak fields. Therefore we use another approximate equation of state²¹ with correct behavior in the weak and strong fields. It can be presented in a convenient form as²²

$$\frac{M}{H_{\text{int}}} = C_0 \left(\frac{\varphi(x)}{\tau} \right)^\gamma \{1 - a[1 - \varphi(x)]\}^{-1}, \quad (2)$$

$$x = h_{\text{int}}/\tau^{\beta_H} = A[1 - \varphi(x)]^{1/2} \{1 - a[1 - \varphi(x)]\} \varphi(x)^{-\beta_H}. \quad (3)$$

Here $A > 0$, $1 > a > 0$ are the coefficients, C_0 is the factor determining the amplitude of χ , $\beta_H = \gamma + \beta$ is the magnetic field index, β is the index of the spontaneous magnetization, $h_{\text{int}} = g\mu H_{\text{int}}/(kT_C)$, and $H_{\text{int}} = H - 4\pi NM$ is the internal field. The function $\varphi(x)$ decreases monotonically from 1 down to 0 as x increases from 0 up to ∞ . The $\varphi(x)$ and, consequently, M/H_{int} are the even functions of x . They can be expanded in the power series in x^2 for $x^2 \ll 1$ because Eq. (3) can be presented as $x^2 = [\text{the right-hand side}]$.² Strongly speaking, a

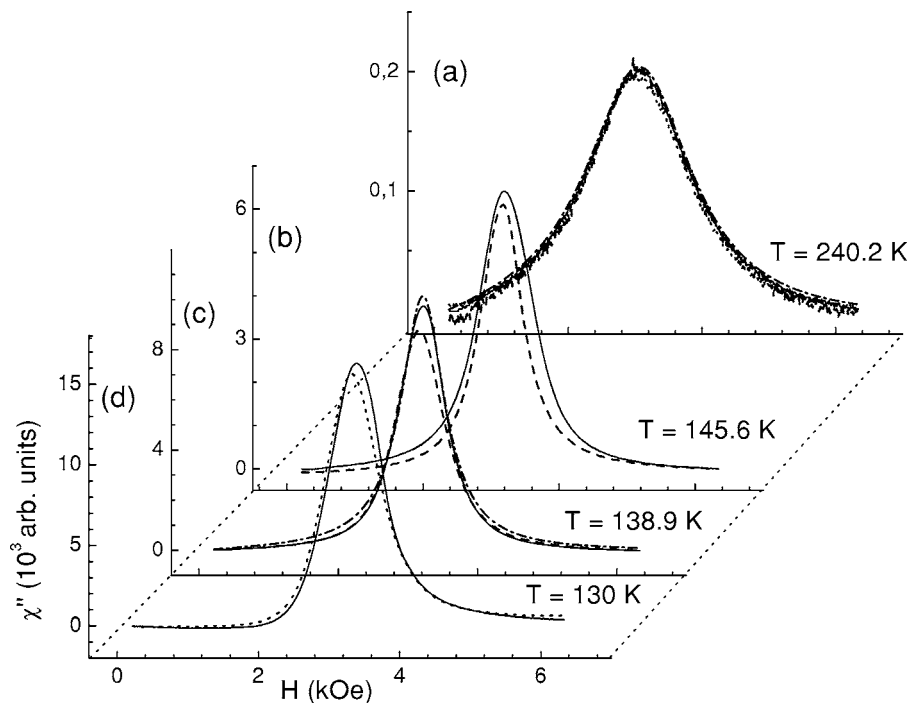


FIG. 4. The ESR spectra for the different T scans at some close temperatures: cooling [solid line, panels (a)–(d)], heating after fast cooling [dashed line, panels (a)–(c)], cooling under $H=4$ kOe [dotted line, panels (a) and (d)]. Panels (a) and (c) also represent the fit of the spectra recorded on cooling by a Lorentzian (dash-dotted line).

$=\gamma/\beta_H$ in this approximation. Nevertheless, the parameters A , a , and β_H (or some of them) can be treated as the free ones at an approximate fit (γ has been determined earlier). Inset (2) in Fig. 3(a) displays the best fit of M/H_{int} at $\gamma \approx 1.39$, $\beta_H \approx 5/3$ (the value for a 3D isotropic ferromagnet), and $N=1/3$ for our sample close to a cube. It gives $a \approx 0.98$ that is not far from the theoretical value $a=\gamma/\beta_H \approx 0.81$. We tried also to find β_H using $a=\gamma/\beta_H$. This yields $\beta_H \approx 1.87$ ($a \approx 0.74$), the fit being worse. These results show that the $M(\tau, H)$ dependence is comparably well-described by the conventional scaling static theory in the anomalous region ($T_C \leq T < T^*$) at $H_{\text{int}} \approx H=1$ kOe. Thus, the anomalous nonlinear critical behavior, that is detected by the M_2 measurements in the low magnetic fields ($H < 100$ Oe), is suppressed by the stronger field. This means also that the anomalous phase occupies a relatively small volume (an upper border does not presumably exceed $1/5$).

According to the FC and ZFC data, $M(H, T)$ exhibits T hysteresis [see Fig. 3(a) and inset in Fig. 3(b)]. This phenomenon is usually observed in the manganates below T_C , whereas its presence above T_C up to 300 K is the unexpected result. The $\delta M(T) = 2(M_{\text{ZFC}} - M_{\text{FC}})/(M_{\text{ZFC}} + M_{\text{FC}})$ exhibits the maximum [$T_{m1} \approx 290$ K, see Fig. 3(b)] at high temperatures between 220 and 300 K which can be attributed to the structural transition occurring in this T range. Below 220 K, δM increases monotonically at $T \rightarrow T_C + 0$. This means that the difference $M_{\text{ZFC}}(T) - M_{\text{FC}}(T)$ is not reduced to a T independent distinguished in the parameters accounting for the $M_{\text{ZFC}}(T)$ and $M_{\text{FC}}(T)$ dependences. One may expect that observation of δM here is related to the two-phase coexistence. The M_2 measurements reveal the two-phase state below $T^* \approx 143$ K as the anomalous nonlinear response becomes larger than the conventional one. Here we use another way for disturbance of the system and analyze another quantity, so that the inhomogeneous magnetic state may be observed

above T^* . For instance, the increasing of δM on cooling below 220 K may reflect the differences in the T dependences of the volume fractions and/or mutual arrangement of the phases. In addition, T^* seems to be also seen in $\delta M(T)$ data as a temperature where $\partial \delta M(T)/\partial T$ has a maximum. At last, $\delta M(T)$ exhibits the maximum at T_C . This corresponds to a conclusion based on the M_2 data¹⁰ that the ordering of both phases occurs simultaneously at T_C . These observations agree with an assumption that formation of the two-phase state takes place independently of the structural transition and does not reduce to the coexistence of the O' and a small amount of the initial O phases.

Note some peculiarities of the T -hysteresis below T_C . According to Fig. 3(a), difference between the FC and ZFC data increases for $T < 90$ K. This agrees with T dependence of the hysteresis loop found in the $\text{Re } M_2(H, T)$ measurements. The modification seems to reflect change in a domain formation. Below 20 K the $M(T)$ exhibits sharp reduction, indicating onset of ordering of the Nd ions whose magnetization is directed antiparallel to that of the Mn moments.

V. ESR

Let us turn to ESR data. Figure 4 shows the typical spectra for some temperatures obtained at different T scans. The similar spectra are also observed for other temperatures above T_C . The spectra recorded at the different treatments coincide well for temperatures above approximately T^* , and are fitted by a Lorentzian line shape,

$$\chi_{as}(\omega, H) = \frac{1}{2} \chi \left\{ \left[\frac{\omega \Gamma}{(\omega - g\mu H)^2 + \Gamma^2} - \frac{\omega \Gamma}{(\omega + g\mu H)^2 + \Gamma^2} \right] \cos \varphi_s - \left[\frac{\omega(\omega - g\mu H)}{(\omega - g\mu H)^2 + \Gamma^2} - \frac{\omega(\omega + g\mu H)}{(\omega + g\mu H)^2 + \Gamma^2} \right] \sin \varphi_s \right\}. \quad (4)$$

Here, χ_{as} is the antisymmetric component of the dynamic susceptibility of the sample, χ is the static susceptibility, ω is the frequency of the ac field, Γ is the relaxation rate of a uniform magnetization, and φ_s is the phase of the signal. Since Γ is rather large, both circularly polarized components of the ac field are taken into account in Eq. (4). Partly for this reason, a control sample (a polycrystalline stable nitroxyl radical with $g=2.055$ and $\Gamma \approx 60$ Oe) is used for tuning a phase of the ac field which is the reference point for φ_s . Besides, an employment of the manganite signal for this tuning will create many problems associated with: (i) a dependence of Γ on temperature; (ii) dependence of φ on H in accordance with the CMR effect; (iii) and a possible deviation of $\chi_{as}(\omega, H)$ from the Lorentzian form due to two previous reasons as well as in consequence of an expected formation of the PS magnetic state in the sample. The fitting parameters in Eq. (4) are Γ , g , φ_s and the amplitude of the signal $A_{as}(T) \propto \chi$.

We consider first a range $T^* - 2T_C$ where the critical behavior follows to that of a 3D isotropic ferromagnet,¹⁰ and the structural refinement does not show any structural transformation. Figure 5 presents the $\Gamma(T)$ and $A_{as}(T)$ dependencies for the different T scans which are obtained between T^* and $2T_C$. It is seen that the different treatments of the sample have little effect on the data. The g factor [$\approx 2.00(1)$] is independent of temperature here. $A_{as}(\tau)$ is expected to obey a scaling law for a 3D isotropic ferromagnet, $A_{as}(\tau) \propto \tau^{-\gamma}$, $\gamma \approx 4/3$, in a weak field regime at $\tau > \tau_H = (g\mu H/kT_C)^{3/5} \approx 3.1 \times 10^{-2}$ for the resonance field $H \approx 3$ kOe. The inset in Fig. 5(b) shows that the $A_{as}(\tau)$ curve follows this prediction down to approximately $\tau \approx 0.11$ and deviates from it at $\tau < 0.11$. This behavior is in reasonable correspondence with that of $\chi(\tau)$ found in the $M(H)$ (see above) and low frequency measurements of the linear response on a weak ac field.¹⁰

Let us go to $\Gamma(\tau)$. In the weakly anisotropic cubic ferromagnets, it is usually given by^{9,23,24}

$$\Gamma(\tau) = \Gamma_c^* \tau^{-1} + \Gamma_{unc}(\tau); \quad \Gamma_{unc}(\tau) = \Gamma_{unc}^* \tau^{4/3} r(\tau). \quad (5)$$

Here Γ_c^* in the critical part of Γ is controlled by the dipolar forces, a single ion anisotropy and anisotropy of the exchange interaction (the latter two appear in the $Pbnm$ symmetry).^{19,25} The term with $\Gamma_{unc}(\tau)$ describes the uncritical contribution including a spin-lattice relaxation rate. The Dzyaloshinsky-Moria interaction also presents in this space group.^{19,25} Following an analysis given in Ref. 26, one can show that this interaction gives contribution to Γ_{unc} only since it connects fluctuations of the magnetization (critical) and staggered magnetization (uncritical). The $\Gamma_{unc}(\tau)$ includes the factors $\tau^{4/3} (\propto \chi^{-1})$ and $r(\tau)$. The latter is the weakly changing function of τ with a finite value at $\tau=0$ that can be chosen $r(0)=1$. This function is known for the relaxation enforced by the anisotropic spin interactions. The matter is that in this case $\Gamma(T) = \Gamma_{unc}(T) \propto [T\chi(T)]^{-1}$ at $T \gg T_C$. The study of a number of manganites where $\Gamma_{unc}(T)$ dominates show that this law is valid at $\tau < 1$ as well.²⁷ It yields $r(\tau) = (1 + \tau)^{-1}$. The $\Gamma(\tau)$ exhibits a critical enhancement at $\tau \rightarrow 0$ below a minimal value at τ_{min} . This behavior is ob-

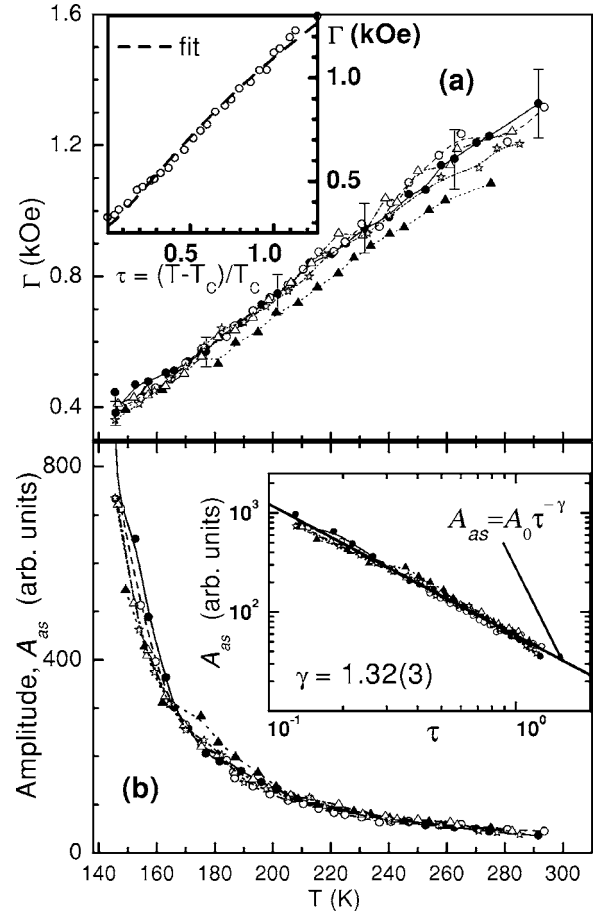


FIG. 5. Temperature dependencies of parameters of the ESR spectra for different T treatments of the sample: cooling (full symbols) and heating (open symbols) under $H=0$ (squares) and $H=4$ kOe (triangles); heating after fast cooling (stars). Panel (a) displays the spin relaxation rate Γ vs temperature. Inset shows $\Gamma(\tau)$ dependence on cooling, and its fit as described in the text. Panel (b) represents amplitudes $A_{as}(T)$ of the spectra vs T . Inset shows fit of $A_{as}(\tau) \propto \chi(\tau)$ to the scaling law.

served in the traditional cubic ferromagnets.¹¹ In our compound $\Gamma(\tau)$ reduces monotonically as $\tau \rightarrow 0$. This dependence can be fitted by the $\Gamma_{unc}(\tau)$ with $r(\tau) = (1 + \tau)^{-1}$ in the range $1.26 > \tau > 0.05$ [see inset in Fig. 5(a)]

$$\Gamma(\tau) = \Gamma_0 + \Gamma_{unc}^* \tau^{4/3} (1 + \tau)^{-1}. \quad (6)$$

The fit gives the following values of parameters: $\Gamma_0 = 282(4)$ and $\Gamma_{unc}^* = 1633(11)$. We find the quasilinear behavior of $\Gamma(\tau)$ as in a number of other manganites near T_C .²⁷ Thus the critical enhancement is not observed, unlike the traditional ferromagnets. This result can be explained by the large uncritical contribution and suppression of the critical enhancement by a magnetic field. It shows a comparison of τ -dependence of the linewidth for our compound with that of cubic ferromagnet CdCr_2Se_4 .¹¹ In the latter Γ_c^* is determined by the dipolar forces $\Gamma_c^* \sim (\omega_d)^2/T_C$, where $\omega_d = 4\pi(g\mu)^2/V_0 \approx 0.4$ K and $T_C \approx 129$ K. Coincidence of T_C and near the same values of ω_d ($\omega_d \approx 0.5$ K in our system) in both ferromagnets suggests the closeness of their critical

dipolar contributions. In CdCr_2Se_4 the $\Gamma_{\text{unc}}^* \sim 40$ Oe is very small compared to that of our compound and is only larger than $\Gamma_C^* \sim 10$ Oe by a factor of 4. As a result, $\Gamma(\tau)$ registered at $\nu \approx 9.21$ GHz revealed all the possible peculiarities: a minimum at $\tau_{\text{min}} \sim 0.3$ due to competition of $\Gamma_C^* \tau^{-1}$ and $\Gamma_{\text{unc}}(\tau)$ as well as the suppression by H of the critical enhancement that leads to formation of a maximum in $\Gamma(\tau)$ at $\tau_{\text{max}} \sim 0.1$.¹¹ The large value of Γ_{unc}^* in our manganite can be attributed to the DM coupling (J_{DM}) that is absent in the cubic ferromagnets and, as noted above, gives contribution to Γ_{unc}^* only. The typical value of this interaction in the manganites belonging to $Pbnm$ space group is $J_{DM} \sim 1$ K.²⁵ A rough estimation $\Gamma_{\text{unc}}^* \sim (zJ_{DM})^2/T_C \approx 2$ kOe ($z=6$ is the coordination numbers of the Mn sublattice) yields the value close to an experimental result.

Let us estimate the critical dipolar contribution in a magnetic field $H, \Gamma_C(\tau, H)$, for our compound. In the weak field regime and an actual resonance case $g\mu H \gg \Gamma$, its H dependence is determined by a spin diffusion mode¹¹

$$\Gamma_C(\tau, H) = \Gamma_C^* \tau^{-1} \{1 - C^*(h/\tau^{5/3})^{1/2}\}, \quad \Gamma_C^* = \omega_d^2/T_C. \quad (7)$$

Here $h = g\mu H/T_C$, $\Gamma_C^* \approx 16$ Oe and $C^* = 0.01 C_\chi^*/C_D^{3/2}$, where C_χ^* is determined by the amplitude of $\chi(4\pi\chi = C_\chi^* \omega_d/T_C)$ and C_D is controlled by the spin diffusion coefficient ($D \propto C_D T_C \tau^{1/3}$). The $\Gamma_C(\tau, H)$ exhibits a maximum as a function of τ . Using $C_D \approx 0.07$ found in CdCr_2Se_4 ,¹¹ we obtain $\tau_{\text{max}} \approx 0.2$ and $\Gamma_C(\tau_{\text{max}}, H) \approx 40$ Oe for resonance field $H \approx 3$ kOe and $C_\chi^* \approx 5.3$ determined above. Thus, in our compound the effect of the dipolar interaction is reduced to the small correction to the large $\Gamma_{\text{unc}} \approx 450$ Oe at $\tau_{\text{max}} \approx 0.2$. Note that the H effect is important since Eq. (5) gives a minimum in $\Gamma(\tau)$ at $\tau_{\text{min}} \approx 0.1$ for $\Gamma_{\text{unc}}^* \approx 1630$ Oe.

The critical contribution of the single ion anisotropy ($J_{\text{an}} S_\alpha^2$) can be also estimated by using Eq. (7) with $\omega_d \rightarrow J_{\text{an}}$. Being related to the distortions of the oxygen octahedra, this interaction is essential below T_{LT} . It is maximal for the strongly distorted LaMnO_3 ($J_{\text{an}} \approx 2$ K)²⁵ and decreases with doping increasing. Taking into account the estimation of the dipolar contribution, we obtain $J_{\text{an}} \leq \omega_d \approx 0.5$ K that agrees with a reduction of this anisotropy in our weakly distorted manganite.

The ESR study of series of manganites with $x \approx 0.33$ (Ref. 27) and $\text{La}_{1-x}\text{Ca}_x\text{MnO}_3$ ($x=0.18 \div 0.22$) (Ref. 28) revealed the strong uncritical relaxation compared to that of our compound. According to our analysis, it is difficult to expect that the critical enhancement can be found in this case. Indeed, the broadening of the ESR line near T_C was found to be sample dependent, and proved to be mainly related to the appearance of a mixed state containing a ferromagnetic phase.^{27,29} The same reason is likely to account for the broadening of the line in the LaCa manganites indicated above since, according to the authors, these compounds exhibited the pure paramagnetic state only in the T range corresponding to the uncritical behavior.

We consider now the ESR data below T^* where a pronounced deviation of the signal from the Lorentzian starts to be observed. A reason is that $\text{Im} 4\pi\chi_{xx}(\omega, H) \gg 1$ at $\omega \approx g\mu H$ as $4\pi\chi \sim 1$ ($4\pi\chi \approx 0.6$ at T^*). This leads to a com-

plex nonuniform distribution of the ac field in the sample because a wave vector k in a medium $k \propto \mu_0 = 1 + 4\pi\chi_{xx}(\omega, H)^{1/2}$ for a wave spreading along \mathbf{H} , where, for simplicity, we neglected the $\chi_{as}(\omega, H)$. As a result, phase φ_s of the signal begins to exhibit a strong H dependence that cannot be correctly determined for our sample in the resonator. Therefore below T^* , we present directly the signals for the several types of the T scans. The pronounced T hysteresis observed in all the measurements (Fig. 4) is the clear indication of the anomalous behavior that develops below T^* . Since a precise quantitative analysis of the signal is not feasible here, we cannot determine whether this hysteresis is caused by that of M or it is related also to hysteresis of the Γ and g factor. A rough estimation gives approximately T -independent values for Γ and g factor below T^* down to T_C . The same reason does not allow us to elucidate a possible two-phase character of the signal. At the same time, above T^* phase φ_s reflects mainly phase shift of the $h(t)$ in the sample which is related to a comparably large $\varepsilon \sim 10$ and conductivity σ . This effect, being independent of H , can be taken into account correctly by Eq. (4). For the largest conductivity [$\sigma \approx 1.7(\Omega\text{cm})^{-1}$] at $T = 2T_C \approx 260$ K, we get $l_\perp |k| \sim 0.25$ for $\mu_0 \approx 1$, where $l_\perp \approx 0.1$ mm is the thickness of the sample. Since σ decreases sharply on cooling [$\sigma \sim 0.3 \times 10^{-2}(\Omega\text{cm})^{-1}$ at T^*], the h distribution in the sample is close to uniform between T^* and $2T_C$.

VI. DISCUSSION AND CONCLUSION

The T hysteresis observed in the magnetization and ESR measurements above T_C evidences at least a weak first order transition. According to the M_2 data, a reason of changing regime of the transition at T^* is formation of the new phase with the anomalous strong nonlinear magnetic behavior in the weak fields which is stronger than that of a 3D isotropic ferromagnet near T_C . This phase coexists with the normal one at least from T^* down to T_C . This PS magnetic state cannot be trivially related to a two-phase structure because, according to the neutron diffraction, the sample remains the structural uniform compound below T^* . Note that, first, the anomalous phase coexists with the conventional one possessing the different orbital ordering for the $x=0.23$ and $x=0.25$ compounds. Second, it arises in the manganites that are closed to border of the I-M transition ($x \approx 0.3$), where, according to Ref. 18 and our preliminary data, the orbital ordering disappears. These observations suggest that the anomalous behavior can be attributed to an orbital disordered metallic phase. The lack of observability of the anomalous phase in the structural measurements means that this phase is structurally close to the conventional one and/or its volume is small. Fragmentation of the sample in the PS state may be such that the anomalous phase does not form a percolative conductive cluster, and the system remains an insulator. The strong H -nonlinear behavior of this phase is expected to be a combined effect of its own properties and a magnetic coupling of its fragments through the normal phase with the developed ferromagnetic correlations. It is very important to stress a difference between this transition and a first order one whose character is determined on the base of $M(H)$ data.

In the latter, type of the transition (first/second) is characterized by the sign of the coefficient b in an expansion of H/M in M^2 above T_C : $H/M = a + bM^2 + \dots$ [$b < 0$ (first order), $b > 0$ (second order)]. Such a criterion suggests that the magnetization is the single critical degree of freedom accounting for the transition. This peculiarity is indeed observed in the $M(H)$ dependence of traditional ferromagnet MnAs (Ref. 30) and a number of the manganites.^{31,32} Besides the conventional $M(H)$ measurements, the sign of b can be found from the M_2 data because $\text{Re}M_2(\omega, H) \propto \partial^2 M / \partial H^2 = -6(b/a^4)H$ for $H \rightarrow 0$ and a small ω when $\text{Re}M_2$ dominates in the response.⁸ Our results on the $x=0.23$ and $x=0.25$ compounds obtained by this method indicate clearly that $b > 0$ for both coexisting phases.^{8,10} This implies that M is not the single degree of freedom involved in the transition, and one should consider the charge, orbital, and JT-phonon variables (or some of

them) as the critical ones as well. It is not the unexpected conclusion for the manganites that are characterized by close interconnection of the magnetization and these degrees of freedom. In our system, the charge and orbital degrees of freedom together with M are the most likely to be the critical variables. The JT-subsystem seems to be less important because the JT distortions are small.

ACKNOWLEDGMENTS

We thank V. I. Voronin for help with magnetization measurements. We are also grateful to V. P. Khavronin for helpful discussions. This work was supported by the joint Russian-Belorussian Foundation for Basic Research, Grant Nos. 04-02-81051 RFBR-Bel2004_a, F04R-076 and partially from the State Program of Neutron Investigation (NI).

-
- ¹I. O. Troyanchuk, D. D. Khalyavin, and H. Szymczak, *J. Phys.: Condens. Matter* **11**, 8707 (1999).
- ²B. B. Van Aken, O. D. Jurchescu, A. Meetsma, Y. Tomioka, Y. Tokura, and T. T. M. Palstra, *Phys. Rev. Lett.* **90**, 066403 (2003).
- ³S. Okamoto, S. Ishihara, and S. Maekawa, *Phys. Rev. B* **61**, 451 (2000).
- ⁴Y. Endoh, K. Hirota, S. Ishihara, S. Okamoto, Y. Murakami, A. Nishizawa, T. Fukuda, H. Kimura, H. Nojiri, K. Kaneko, and S. Maekawa, *Phys. Rev. Lett.* **82**, 4328 (1999).
- ⁵T. V. Ramakrishnan, H. R. Krishnamurthy, S. R. Hassan, and G. Venketeswara Pai, *Phys. Rev. Lett.* **92**, 157203 (2004).
- ⁶P. Dai, J. A. Fernandez-Baca, E. W. Plummer, Y. Tomioka, and Y. Tokura, *Phys. Rev. B* **64**, 224429 (2001).
- ⁷I. D. Luzyanin, V. P. Khavronin, V. A. Ryzhov, I. I. Larionov, and A. V. Lazuta, *Pis'ma Zh. Eksp. Teor. Fiz.* **73**, 369 (2001) [*JETP Lett.* **73**, 327 (2001)].
- ⁸V. A. Ryzhov, A. V. Lazuta, I. D. Luzyanin, I. I. Larionov, V. P. Khavronin, Yu .P. Chernenkov, I. O. Troyanchuk, and D. D. Khalyavin, *Zh. Eksp. Teor. Fiz.* **121**, 678 (2002) [*JETP* **94**, 581 (2002)].
- ⁹V. A. Ryzhov, A. V. Lazuta, I. A. Kiselev, Yu .P. Chernenkov, O. P. Smirnov, S. A. Borisov, I. O. Troyanchuk, and D. D. Khalyavin, *Solid State Commun.* **128**, 41 (2002).
- ¹⁰V. A. Ryzhov, A. V. Lazuta, V. P. Khavronin, I. I. Larionov, I. O. Troyanchuk, and D. D. Khalyavin, *Solid State Commun.* **130**, 803 (2004).
- ¹¹V. N. Berzhansky, V. I. Ivanov, and A. V. Lazuta, *Solid State Commun.* **44**, 77 (1982).
- ¹²D. D. Khalyavin, M. Pekala, G. L. Bychkov, S. V. Shiryayev, S. N. Barilo, I. O. Troyanchuk, J. Mucha, R. Szymczak, M. Baran, and H. Szymczak, *J. Phys.: Condens. Matter* **15**, 925 (2003).
- ¹³A. G. Soldatov, S. V. Shiryayev, and S. N. Barilo, *J. Analytic. Chem.* **56**, 1077 (2001).
- ¹⁴V. A. Ryzhov, E. I. Zavatskii, V. A. Solov'ev, I. A. Kiselev, V. N. Fomichev, and V. A. Bikineev, *Zh. Tekh. Fiz.* **65**, 133 (1995) [*Tech. Phys.* **40**, 71 (1995)].
- ¹⁵V. A. Ryzhov, A. V. Lazuta, I. A. Kiselev, I. D. Luzyanin, and T. I. Arbuzova, *Zh. Eksp. Teor. Fiz.* **117**, 387 (2000) [*JETP* **90**, 341 (2000)].
- ¹⁶T. Chatterji, B. Ouladdiaf, P. Mandal, B. Bandyopadhyay, and B. Ghosh, *Phys. Rev. B* **66**, 054403 (2002).
- ¹⁷Q. Huang, A. Santoro, J. W. Lynn, R. W. Erwin, J. A. Borchers, J. L. Peng, K. Ghosh, and R. L. Greene, *Phys. Rev. B* **58**, 2684 (1998).
- ¹⁸F. Fauth, E. Suard, C. Martin, and F. Millange, *Physica B* **241-243**, 427 (1998).
- ¹⁹J. Deisenhofer, B. I. Kochelaev, E. Shilova, A. M. Balbashov, A. Loidl, and Krug H.-A. von Nidda, *Phys. Rev. B* **68**, 214427 (2003).
- ²⁰H. Kaiser, L. E. Stumper, J. J. Rhyne, Y. Tokura, and H. Kuwahara, *J. Appl. Phys.* **85**, 5564 (1999).
- ²¹A. Z. Patashinskii and V. L. Pocrovskii, *Fluctuation Theory of Phase Transitions* (Pergamon, Oxford, 1980).
- ²²A. V. Lazuta, I. I. Larionov, and V. A. Ryzhov, *Zh. Eksp. Teor. Fiz.* **100**, 1964 (1991) [*Sov. Phys. JETP* **73**, 1086 (1991)].
- ²³D. L. Huber, *J. Phys. Chem. Solids* **32**, 2145 (1971).
- ²⁴S. V. Maleev, *Sov. Sci. Rev., Sect. A* **8**, 1229 (1987).
- ²⁵D. L. Huber, G. Alejandro, A. Caneiro, M. T. Causa, F. Prado, M. Tovar, and S. B. Oseroff, *Phys. Rev. B* **60**, 12155 (1999).
- ²⁶A. V. Lazuta, *Physica C* **181**, 127 (1991).
- ²⁷M. T. Causa, M. Tovar, A. Caneiro, F. Prado, G. Ibañez, C. A. Ramos, A. Butera, B. Alascio, X. Orbadós, S. Piñol, F. Rivadulla, C. Vázquez-Vázquez, A. López-Quintela, J. Rivas, Y. Tokura, and S. B. Oseroff, *Phys. Rev. B* **58**, 3233 (1998).
- ²⁸A. I. Shames, E. Rozenberg, G. Gorodetsky, and Ya. M. Mukovskii, *Phys. Rev. B* **68**, 174402 (2003).
- ²⁹F. Rivadulla, L. E. Hueso, M. A. López-Quintela, J. Rivas, and M. T. Causa, *Phys. Rev. B* **64**, 106401 (2001).
- ³⁰P. Bean and D. S. Rodbell, *Phys. Rev.* **126**, 104 (1962).
- ³¹J. Mira, J. Rivas, F. Rivadulla, C. Vázquez-Vázquez, and M. A. López-Quintela, *Phys. Rev. B* **60**, 2998 (1999).
- ³²C. S. Hong, W. S. Kim, and N. H. Hur, *Phys. Rev. B* **63**, 092504 (2001).